

TEXTBOOK

Antonio Pulido-Bosch

Principles of Karst Hydrogeology

Conceptual Models, Time Series
Analysis, Hydrogeochemistry
and Groundwater Exploitation



Springer

Springer Textbooks in Earth Sciences, Geography and Environment

The Springer Textbooks series publishes a broad portfolio of textbooks on Earth Sciences, Geography and Environmental Science. Springer textbooks provide comprehensive introductions as well as in-depth knowledge for advanced studies. A clear, reader-friendly layout and features such as end-of-chapter summaries, work examples, exercises, and glossaries help the reader to access the subject. Springer textbooks are essential for students, researchers and applied scientists.

More information about this series at <http://www.springer.com/series/15201>

Antonio Pulido-Bosch

Principles of Karst Hydrogeology

Conceptual Models, Time Series
Analysis, Hydrogeochemistry
and Groundwater Exploitation

Antonio Pulido-Bosch
University of Granada
Granada, Spain

ISSN 2510-1307 ISSN 2510-1315 (electronic)
Springer Textbooks in Earth Sciences, Geography and Environment
ISBN 978-3-030-55369-2 ISBN 978-3-030-55370-8 (eBook)
<https://doi.org/10.1007/978-3-030-55370-8>

© Springer Nature Switzerland AG 2021

This work is subject to copyright. All rights are reserved by the Publisher, whether the whole or part of the material is concerned, specifically the rights of translation, reprinting, reuse of illustrations, recitation, broadcasting, reproduction on microfilms or in any other physical way, and transmission or information storage and retrieval, electronic adaptation, computer software, or by similar or dissimilar methodology now known or hereafter developed.

The use of general descriptive names, registered names, trademarks, service marks, etc. in this publication does not imply, even in the absence of a specific statement, that such names are exempt from the relevant protective laws and regulations and therefore free for general use.

The publisher, the authors and the editors are safe to assume that the advice and information in this book are believed to be true and accurate at the date of publication. Neither the publisher nor the authors or the editors give a warranty, expressed or implied, with respect to the material contained herein or for any errors or omissions that may have been made. The publisher remains neutral with regard to jurisdictional claims in published maps and institutional affiliations.

This Springer imprint is published by the registered company Springer Nature Switzerland AG
The registered company address is: Gewerbestrasse 11, 6330 Cham, Switzerland

Preface

This book is an attempt, from an essentially hydrogeological point of view, to bring together both traditional and more recent concepts relating to karst landscapes. If we are not to overlook the fundamental scientific aspects, this is the only most practicable approach.

Karst material has always aroused a great deal of interest due to its unique character and its huge economic importance, and also because the terrain that it creates often permits us to embark on underground exploration. This has been a major attraction over the years for all who love hidden things and is why the early scientific contributions had an exploratory component of the unknown, the underground world. Classical works are Martel's *Les abîmes*, Llopis' posthumous book and numerous journals around the world that disseminated the more or less sporting results of the exploits of many hardworking speleologists. Journals such as *Lapiaz* and *Spelunka* are among many that supported thousands of topographic surveys and records. The International Speleological Union (UIS) brought together illustrious sportsmen and women who loved the subterranean world, as well as scientists passionate about the land's depths, to engage in activities that are not without risk and that have left many behind in the caverns and passages that they so wanted to discover.

Scientists have entered fully into this exciting domain, investigating morpho-dynamic, morphogenetic and hydrogeological aspects in not only theoretical but also highly applied research. Karst water has a clear economic interest and is often the best—or only—source of urban water supply. The International Association of Hydrogeologists has been active in this regard, founding the Commission for Karst Hydrogeology. This has published numerous core reference works and organized milestone events in the advancement of this unique field of science. The Dubrovnik Colloquium (1966) initiated the series that continued in meetings in Antalya (Turkey), Besançon and Neuchâtel, alternating for two decades, also in Nerja and Malaga. More details can be found at <http://www.iah.org/karst/>, <http://www.speleogenesis.info/>, <http://www.karstportal.org/>, <http://karstwaters.org/>, <http://nckri.org/>, <http://www.karst.edu.cn>, <http://www.irck.edu.cn> and <http://www.sedeck.org/>.

Much of this information, together with research by numerous centres (Laboratoire Souterrain de Moulis of the CNRS, University of Neuchâtel, and Granada, Besançon, Montpellier and Malaga Universities), has formed the basis of this work,

which aims to serve as a route into the exciting world of karst hydrogeology. It aims to provide a foundation that I hope will help the interested graduate to come to know better its characteristics, the parameters of interest and their quantification and the means for exploration, acting as a solid base of knowledge on capturing and exploiting this water resource. This volume also details the physical and chemical characteristics of karst water and specifies how it may be protected from contamination.

This book is the result of many years of dedication to the study of the hydrogeology of karst, at first in a personal way and later with the decisive support of numerous collaborators, some of them already university professors and other professionals. My work has benefited from a wide range of funding, both public and competitive—national, regional and European—as well as research contracts of many types.

Degree Theses

- Benavente, J. 1978. *Hydrogeological research in the Sierra de Jaen*.
- Casares, J. 1978. *Hydrogeological investigations in the karstic massifs of Parapanda and Hacho de Loja (province of Granada)*.
- Fernández, R. 1980. *Hydrogeological investigations to the North of Ronda (Málaga)*.
- Moreno, I. 1981. *Contribution to the hydrogeological knowledge of the Sierras de Maria and Maimon (province of Almería)*.
- Obartí, F.J. 1986. *Systems analysis applied to karst hydrogeology*.
- Calaforra, J.M. 1987. *Hydrogeology of the karstified gypsum of Sorbas (province of Almería)*.
- Molina, L. 1989. *Contribution to the hydrogeochemical knowledge of the eastern sector of Campo de Dalías (Almería)*.
- López-Chicano, M. 1989. *Geometry and structure of a perimediterranean karstic aquifer: Sierra Gorda (Granada and Malaga)*.

Doctoral Theses

- Padilla, A. 1990. *Application of mathematical models to the study of karstic aquifers*.
- Navarrete, F. 1992. *Contribution to the hydrogeochemical knowledge of Campo de Dalías*.
- López-Chicano, M. 1992. *Contribution to the knowledge of the karstic hydrogeological system of Sierra Gorda and its surroundings (Granada and Malaga)*.
- Calaforra, J.M. 1996. *Contribution to the knowledge of gypsum karstology*.
- Martín-Rosales, W. 1997. *Effects of the check-dams on the southern edge of the Sierra de Gádor (Almería)*.
- Andreu, J.M. 1997. *Contribution of overexploitation to the knowledge of the karstic aquifers of Crevillente, Cid and Cabeço d'Or (province of Alicante)*.
- Vallejos, A. 1997. *Hydrogeochemical characterization of the recharge of the Campo de Dalías aquifers from the Sierra de Gádor (Almería)*.
- Molina, L. 1998. *Hydrochemistry and marine intrusion in Campo de Dalías (Almería)*.
- El Morabití, K. 2000. *Contribution to the geological, hydrochemical and isotope knowledge of the thermal waters of northern Morocco*. Univ. Abdelmalek Essaadi, Tetouan.

- Contreras, S. 2006. *Spatial distribution of the annual water budget in semi-arid mountain regions. Application in Sierra de Gádor (Almería)*.
- Daniele, D. 2007. *Application of geographic information systems to the study of complex aquifers. Case of Campo de Dalías*.

Finally, I list the main research projects with which I have been involved, as well as the most relevant contracts.

Research Projects and Contracts

- Mathematical models applied to the analysis of karst aquifers*. CAICYT, 1983–1987.
- Overexploitation in karstic aquifers*. DGICYT. 1988–1992.
- Hydrogeological aspects of groundwater protection in karst areas*. CICYT. 1992–1995.
- Characterization of contaminating processes in karstic aquifers*. CICYT. 1995–1998.
- Hydrogeological characterization of karst aquifers in semi-arid regions. The case of the Turón–Sierra de Gádor macrosystem*. PO6-RNM-01696 Consejería de Innovación, Junta Andalucía, 2007–2010.
- Action COST–65. *Hydrogeological aspects of the protection of groundwaters in karstic areas, 1991–1995*. 16 European countries.
- Analysis and modelling of the elements of karst springs with a view to their characterization and forecasting of temporal evolution*. Hispano–Bulgarian Project (CSIC—Bulgarian Academy of Sciences). 1991.
- Comparative analysis of karst aquifer structures*. Hispano–Bulgarian Project (CSIC—Bulgarian Academy of Sciences). 1992.
- Mathematical simulation of the karstic coastal aquifers of Pinar del Río, Havana and Matanzas (Cuba)*. Institute for Ibero-American Cooperation (ICI).
- CNIC Ministry of Higher Education, Cuba. 1994. *Mathematical simulation of the coastal aquifer of Zapata, province of Matanzas, Cuba*. ICI. CNIC. 1995.
- Les Rencontres Méditerranéennes du Karst*, EU, DG XI/A/2 France, Portugal and Spain. 1995.
- Ecological problems of karst waters caused by overexploitation and contamination (on the example of North-East Bulgaria)*. CIPACT930139, UE, COPERNICUS. National Institute of Meteorology and Hydrology, School of Mines, and Hydrocomp Ltd, Sofia, Bulgaria. 1994–1997.
- Groundwater karst systems: Conceptual modelling and evaluation of their vulnerability*. EST. CLG975809 NATO. National Institute of Meteorology and Hydrology in Sofia, Bulgaria. 1999–2001.
- Monitoring and densification of the retention check dams on the southern edge of the Sierra de Gádor and analysis of their influence on the environment*. Contract IARA—University of Granada. 1990–1993.
- Hydrogeological study of the Fuente del Rey (Manantial de la Salud) and its surroundings (Priego de Córdoba)*. University of Granada–Priego de Córdoba Town Hall. 1992.
- Hydrogeochemical study of the aquifer systems of the South of the Sierra de Gádor–Campo de Dalías*. Contract Cajamar—University of Almería. 2001–2002.
- Evaluation of recharge and proposals to increase infiltration in the aquifers of the South of the Sierra de Gádor–Campo de Dalías*. Contract Cajamar—University of Almería. 2001–2002.
- The hydrogeological problem of the Valle de Abdalajís Tunnel and its surroundings*. Contract U.T. E. Ayegeo Abdalajís—University of Almería. 2005–2006.
- Hydrogeological advisory services for underground works on the High-speed South line*. Contract ADIF—Universidad Almería. 2009–2012.
- 41986, n° 6/52, *Research on the karstic hydrogeology of carbonate massifs*. C. Romariz (U. Lisboa) and A. Pulido-Bosch (U. Granada).

- 1991, *Comparison of hydrogeological and hydrogeochemical aspects in karstic aquifers linked to gypsum*. P. Forti (U. Bologna) and A. Pulido-Bosch (U. Granada).
- 1991, *Quantitative approach to karst hydrogeology. Comparative study of some Pyrenean and Betic karsts*. G. de Marsily (U. Pierre and Marie Curie, Paris) and A. Pulido-Bosch (U. Granada).
- 1991, *Comparative analysis of the structures of karstic aquifers*. C. Drogue (USTL, Montpellier) and A. Pulido-Bosch (U. Granada).
- 1991, Hispano–Bulgarian bilateral project *Analysis and modelling of the elements of karst springs with a view to their characterization and forecasting of temporal evolution*. D. Dimitrov (Institute of Meteorology and Hydrology, Bulgarian Academy of Sciences, Sofia) and A. Pulido-Bosch (IAGM, CSIC).
- 1992, Spanish–Bulgarian bilateral project *Comparative analysis of karst aquifer structures* (CSIC—Bulgarian Academy of Sciences).

My good speleologist friends have helped me so much at various points in my professional career: among others, Juan de Dios Pérez Villanueva, doctor in Geography and firefighter; and Toni Fornes, who provided me with numerous photographs of the Vallada area for this book, to mention just two especially representative of this generous group of individuals who love karst so much. The final phase of the book was written in the Department of Geodynamics of the University of Granada during a long personal stay that had the support of the members of the department, especially Profs. Calvache and Azañón. I wish to express my sincere gratitude to them all for their remarkable efforts and the sincere friendship that they have always extended to me.

This work would not have been possible without the continued help of Paule Leboeuf Gaborieau over many years and his enormous effort in adapting all the figures that are included in this book. It is clear that this is a joint work. Thank you so very much.

Finally, I would like to acknowledge the contribution of Dr. Alexis Vizcaino (Springer Nature) and Alison Williamson (Burgess Pre-Publishing) editing this textbook. The English edition is based on *Principios de Hidrogeología kárstica*, published by Editorial Universidad de Almería in Spanish in 2015.

Granada, Spain
March 2020

Antonio Pulido-Bosch

Contents

1 Karst and Pseudokarst Materials	1
1.1 Glossary	1
1.2 General Aspects	2
1.3 Classification and Composition of Karst Materials	2
1.4 Porosity and Permeability in Carbonate Rock	5
1.4.1 General Aspects	5
1.4.2 Porosity and Permeability in Dolomites	6
1.5 Porosity and Permeability in Matrix	10
1.6 Fracture Analysis	10
1.6.1 Basic Concepts	10
1.6.2 Box 1: Olkusz Region (Poland)	12
1.6.3 Box 2: Betic Cordillera	20
1.6.4 Box 3: Sector North of Ronda	24
1.6.5 Box 4: Sorbas Gypsum	34
1.6.6 Box 5: Sierra Gorda	39
1.7 Further Reading	51
1.8 Short Questions	51
1.9 Personal Work	52
References	52
2 Karstification and Forms	55
2.1 Glossary	55
2.2 Karstification	56
2.2.1 Corrosion	56
2.2.2 Dissolution of Hypersoluble Rocks	58
2.2.3 Erosion	58
2.2.4 Insoluble Substances	59
2.3 Forms Resulting from Corrosion and Incrustation	60
2.3.1 Main Forms	60
2.4 Box 1: Sorbas Karst	63
2.4.1 The Karst Forms	64
2.4.2 Hydrogeological Aspects	70
2.5 Box 2: Gypsum Karst of Vallada (Valencia)	71

2.6	Box 3: Pseudokarst Forms on the Southern Edge of Sierra del Maimón (Almería)	76
2.7	Box 4: The Pinoso Karst (Alicante)	79
	2.7.1 Geomorphological Aspects	83
	2.7.2 Hydrogeology	84
2.8	Further Reading	88
2.9	Short Questions	89
2.10	Personal Work	89
	References	90
3	Conceptual Models of Karst Aquifers	93
3.1	Glossary	93
3.2	General Aspects	94
3.3	Conceptual Models	94
	3.3.1 General Characteristics	94
3.4	Box 1: Data to Build a Conceptual Model	98
	3.4.1 Characteristics of Boreholes	98
	3.4.2 Factors Influencing the Structure of Aquifers	104
3.5	Box 2: Typology of Aquifers in Carbonate Rock	105
3.6	Further Reading	107
3.7	Short Questions	107
3.8	Personal Work	108
	References	108
4	Analysis of Hydrographs	111
4.1	Glossary	111
4.2	Introduction	111
	4.2.1 General Aspects	111
	4.2.2 Depletion or Base Flow	112
	4.2.3 Recession	116
4.3	Identification of Flow Modalities	116
	4.3.1 Background	116
4.4	Box 1: Application of Classical Methodology	120
	4.4.1 Depletion Graph Analysis	122
4.5	Mangin's Equation	131
	4.5.1 Box 2: Application of Mangin's Equation	135
4.6	Coutagne's Equation	139
	4.6.1 Theoretical Development	139
	4.6.2 Box 3: Application of Coutagne's Equation	141
4.7	Further Reading	144
4.8	Short Questions	145
4.9	Personal Work	145
	References	145

5	Time Series Analyses	147
5.1	Glossary	147
5.2	Introduction	147
5.3	Correlation and Spectral Analysis	148
5.3.1	Simple Analysis	148
5.3.2	Cross-Analysis	149
5.3.3	Using Correlation and Spectral Analysis	152
5.3.4	Cross-Analysis	153
5.3.5	Applications	159
5.3.6	Linearity	161
5.4	Box 1: Worked Examples of Cross-Analysis	165
5.4.1	Torcal de Antequera	165
5.4.2	Sierra Grossa	165
5.4.3	Procedures Undertaken	166
5.5	Box 2: Comparison to Systems in the French Pyrenees	173
5.6	Box 3: The Alfaro-Medioldía-Segaria Unit	177
5.7	Box 4: Applying the Methods to Bulgarian Springs	181
5.7.1	Hydrogeological Characteristics of the Areas Studied	181
5.7.2	Simple Correlation and Spectral Analysis	186
5.7.3	Cross-Spectral Analysis	190
5.8	Further Reading	192
5.9	Short Questions	192
5.10	Personal Work	193
	References	193
6	Mathematical Models	195
6.1	Glossary	195
6.2	General Aspects	196
6.3	Black-Box Models	196
6.3.1	Convolution and Deconvolution	197
6.3.2	Tank Models	197
6.4	The AR, MA, ARMA and ARIMA Processes	201
6.4.1	ARIMA Models	201
6.4.2	Univariate ARMA Models	204
6.4.3	Box 1: Application of Black-Box Models	207
6.4.4	Box 2: Application of ARMA Models	219
6.4.5	Box 3: Application of Traditional Models	224
6.5	'Traditional' and Specific Models	236
6.5.1	General Aspects	236
6.6	Further Reading	237
6.7	Short Questions	238
6.8	Personal Work	238
	References	239

7	Hydrogeochemistry and Water Quality	241
7.1	Glossary	241
7.2	Theoretical Considerations	242
7.2.1	Limestone and Dolomite Waters	242
7.2.2	Data Presentation	244
7.3	Examples of Hydrogeochemical Studies	246
7.3.1	Box 1: Saline Springs of Sierra de Mustalla (Valencia)	246
7.3.2	Box 2: Salado Springs (Sierra Gorda, Granada)	253
7.3.3	Box 3: Sierra de Gádor, Pilot Area	257
7.3.4	Box 4: The Crevillente Aquifer	275
7.3.5	Box 5: Sorbas Gypsum	282
7.3.6	Box 6: Hydrogeochemistry of the Vallada Area (Valencia)	284
7.3.7	Box 7: Salt Evaporites of Fuente Camacho	285
7.4	Pollution and Potential Sources	296
7.4.1	Background	296
7.4.2	Hazards in Karst Groundwater	297
7.4.3	Developing Protection Procedures	304
7.5	Further Reading	309
7.6	Short Questions	310
7.7	Personal Work	310
	References	311
8	Exploration and Exploitation	313
8.1	Glossary	313
8.2	Background	314
8.3	Exploration Methods	316
8.3.1	General Considerations	316
8.3.2	Morpho-Structural Analysis	318
8.3.3	Geophysical Methods	318
8.3.4	Hydrodynamic Methods	320
8.3.5	Infiltration Recharge and Distribution	325
8.3.6	Hydrogeochemistry and Tracers	329
8.3.7	Simulation Models	341
8.4	Exploitation Methods	341
8.4.1	Background	341
8.4.2	Diversion of Springs	343
8.4.3	Reservoirs Formed Within Springs	346
8.4.4	Galleries	346
8.4.5	Boreholes	349
8.4.6	Other Exploitation Systems	357

8.5	Impacts of Exploitation	360
8.5.1	Direct Impacts	360
8.5.2	Indirect Impacts	362
8.6	Further Reading	365
8.7	Short Questions	365
8.8	Personal Work	366
	References	366



Karst and Pseudokarst Materials

1

1.1 Glossary

Karst has two meanings: the first is synonymous with *karst region*, one made up of carbonate, compact and soluble rocks that display characteristic surface and underground forms; the other, by extension, refers to any effect of karstification on karstifiable rock.

Pseudokarst alludes to a region that presents forms analogous to those of karst in rock that is only slightly or not at all karstifiable (subject to karstification).

Karst phenomena refer to all karst forms and the processes that determine them; the latter comprise *karstification*.

Karst material is material from *karst*; in the wider sense, it is used to refer also to *pseudokarst* and *thermokarst* material.

Microscopic voids between minerals create *intercrystalline porosity* of 0.1 to 1% of the rock's total porosity. The voids between cemented grains are *interstitial porosity*. Both can be referred to as *matrix porosity*, as opposed to *conduit porosity*.

Macroscopic porosity refers to large karstified fractures, conduits, channels and caves; a specific case is *cavernous porosity*, when large holes of karst origin predominate.

Dolomitization is mole-by-mole replacement of the calcium in a limestone by magnesium, which results in a volume reduction of about 13% as the dolomite is denser than calcite (2.866 against 2.718 g/cm³). This leads to an increase in the porosity of the resulting dolomitic rock. This type of *dolomitization* porosity is *intercrystalline*.

Interconnected porosity (P_o) is the total volume of interconnected pores, effectively equivalent to total porosity.

Relative drainability equates to $S_o = S/P_o$, the quotient of a rock's storage coefficient (S) and its coefficient of open porosity (P_o).

1.2 General Aspects

The term ‘karst’ derives from the region between Trieste and Ljubljana (Laibach), as it formerly belonged to the Austro-Hungarian Empire (Karst, until 1918), then Italy (Carso, until 1945), Yugoslavia and present-day Slovenia (Kras). This area has similar characteristics all along the eastern Adriatic (Istria, Croatia and Dalmatia) and is comprised of limestone with peculiar morphological and hydrological features. From a hydrological point of view, karst areas have an almost total absence of surface drainage, and they feature both endorheic basins and considerable groundwater circulation.

Classically, the term **karst** has two meanings. One is synonymous with karst region, a *region constituted of carbonate, compact and soluble rock with characteristic surface and underground forms*; the other, by extension, refers to the effect of karstification on a karstifiable rock. The term may also be applied to any region constituted of a soluble rock (gypsum and salt), for which some authors reserve the term **pseudokarst**, defined as a *region that presents forms analogous to those of karst in a rock that is only slightly or not at all karstifiable* (or the effects of karstification in such material). The concept of a **karst phenomenon** applies to both karstic forms and the processes that make them; the latter comprise **karstification**.

The importance of carbonate rock is clear from the fact that it represents around 5% in volume of the Earth’s lithosphere. The percentage of carbonate rock of all sedimentary rock is approximately 15%. Carbonates predominate among relatively recent formations, because these are mainly organic sediments. Thus, we can estimate that approximately, 12% of the continental surface is comprised of carbonate rock. About 25% of the world’s population is supplied by karst water [1–3]. In Europe, carbonate outcrops make up over 3 Mkm² (35%) of the land. Figure 1.1 shows the main expanses on both sides of the Mediterranean.

Spain’s limestone regions cover about 100,000 km² (Fig. 1.2): 17,000 km² in the Cantabrian Cordillera, the Basque Country and the Pyrenees; 48,000 km² in the Iberian Cordillera; 7500 km² in the Catalan Cordillera; and 30,500 km² in the Betic Cordillera [4, 5]. It is estimated that the average annual hydrological recharge is 20,000 hm³, while the reserves can exceed 200,000 hm³, hence their enormous economic and ecological interest.

1.3 Classification and Composition of Karst Materials

A classic classification of *karst material* in *s. l.* is as follows (Table 1.1).

From both practical and economic points of view, karst material in its narrow sense is of most interest. Hypersoluble karst material will also be described—specifically gypsum, since the remaining substances are studied by other fields. The limestones and dolomites that constitute carbonate rock are karst material par excellence. The marls, a mixture of carbonate and clay, are of little interest as aquifers. The four aspects of a carbonate rock usually considered are: its chief

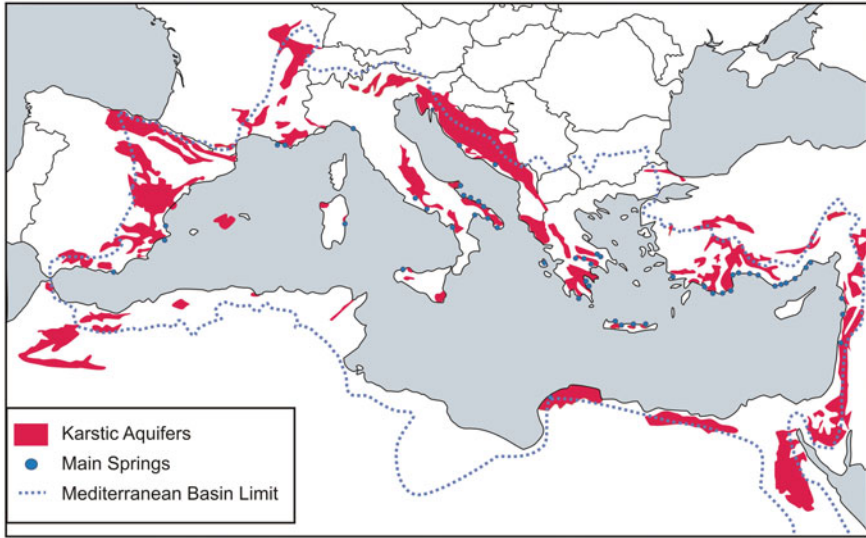


Fig. 1.1 Main outcrops of carbonate materials in the Mediterranean Basin (Adapted from [6])

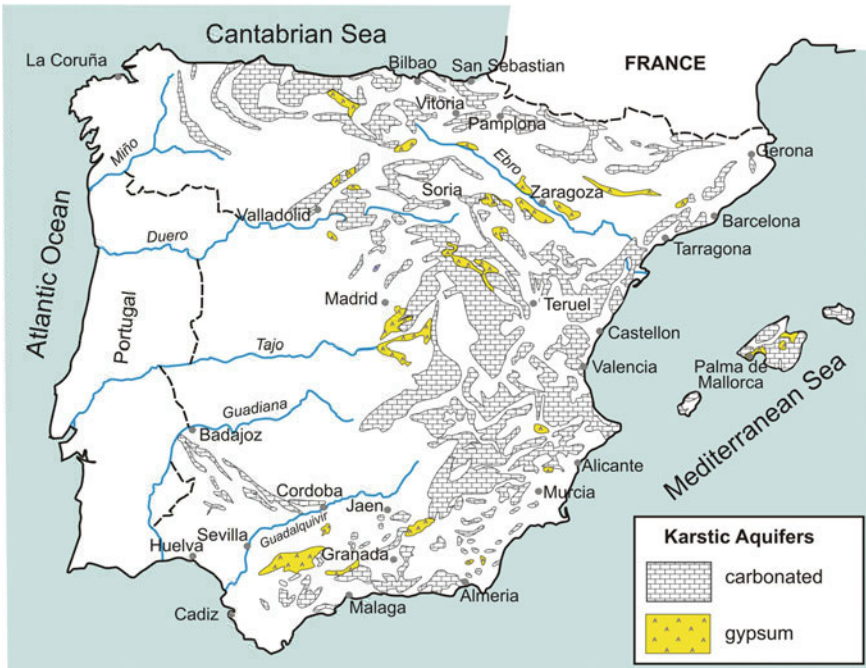


Fig. 1.2 Main outcrops of karst materials in Spain (Adapted from [7])

Table 1.1 Division of karst materials

Karst material (<i>s. str.</i>)	<ul style="list-style-type: none"> ┌ Limestone ├ Dolomite └ Marble 	
Pseudokarst material	<ul style="list-style-type: none"> ┌ Detrital ├ Hypersoluble^(a) (evaporites) └ Hyposoluble^(a) 	<ul style="list-style-type: none"> ┌ soluble cement └ clay matrix
Thermokarst material	<ul style="list-style-type: none"> ┌ Ice masses └ Frozen formations 	

^aWith regard to limestone
Adapted from [8]

element; its minority and trace elements; its fluid inclusions; and its non-carbonate components. The main minerals are calcite, dolomite and gypsum, but there are many others (Table 1.2).

As the radius of Ca^{2+} is 0.99 Å and Mg^{2+} is 0.66 Å, the substitution of one for the other leads to a considerable change in a rock's volume. Further carbonates are able to make isomorphic substitutions with the chief mineral yet do not constitute rock themselves, such as ankerite ($\text{CaFe}(\text{CO}_3)_2$), siderite (FeCO_3), rhodochrosite (MnCO_3) and witherite (BaCO_3).

Minor elements and traces are those that make up just a small fraction of the total constituents. The following elements can replace a mineral's main constituent element. In calcite, Ca can be replaced by: Mg, Mn, Fe^{2+} , Sr, Ba, Co, Zn. In aragonite, Ca can be replaced by: Sr, Pb, Ba, Mg, Mn. Dolomite is a double carbonate of Ca and Mg: its Mg can be replaced by Fe, Mn, Pb, Co, Ba, Zn, Ca; and its Ca can be replaced by: Mn, Fe, Pb and Al.

Table 1.2 Main elements in karst rock, showing their characteristics

Mineral	Density	Composition	System
Calcite	2.71	CaCO_3	Trigonal
Aragonite	2.94	CaCO_3	Rhombic
Dolomite	2.87	$\text{MgCa}(\text{CO}_3)_2$	Hexagonal
Magnesite	3.06	MgCO_3	Hexagonal
Gypsum	2.32	$\text{CaSO}_4 \cdot 2\text{H}_2\text{O}$	Monoclinic
Anhydrite	2.95	CaSO_4	Rhombic
Polyhalite	2.78	$\text{K}_2\text{Ca}_2\text{Mg}(\text{SO}_4)_4 \cdot 2\text{H}_2\text{O}$	Triclinic
Halite	2.16	NaCl	Cubic
Silvinite	1.99	KCl	Cubic
Carnalite	1.6	$\text{KCl} \cdot \text{MgCl}_2 \cdot 6\text{H}_2\text{O}$	Rhombic

Inclusions, on the other hand, can be detected under the electron microscope in the form of tiny bubbles or droplets. When abundant, these give a spongy appearance to certain calcites. The droplets may contain Na^+ , K^+ , Cl^- , together with Ca^{2+} , Mg^{2+} and SO_4^- , besides gases such as CO_2 and CH_4 . Under certain conditions, their study yields valuable information on the genesis of the minerals and the environmental conditions, hence is of interest when prospecting for mineral deposits and undertaking palaeoclimatic reconstruction.

Of the *non-carbonate components*, the clay fraction is the most plentiful and significant impurity; silica is also abundant, both of detrital origin and chemical precipitation (nodules or strata). Other non-carbonate minerals that may be present are: fluorite, celestine, zeolite, goëtitite, barite, phosphate, pyrolusite, gypsum, stroncyanite, feldspar, mica, quartz, rutile, glauconite—also chlorite—tourmaline and pyrite-marcasite. This explains the presence of these ions in solution, not necessarily due to contamination.

The minerals listed above are the main ones seen in karstification and likely to be found in karst caves, but the actual list is much longer. Hill and Forti [9] have edited an interesting collection of slides of the very wide range minerals found in caverns and speleothems.

1.4 Porosity and Permeability in Carbonate Rock

1.4.1 General Aspects

The high porosity of a carbonate mud is reduced to a tiny fraction of its original by diagenesis, in consequence of the processes of compaction, cementation and recrystallization, from 5 to 15% of total porosity in the most favourable cases. Its permeability, according to investigations in hydrocarbon prospecting, will also be very low; the highest values are in calcarenite and calcirrudite with little cementation and in highly recrystallized dolomite, at between 10^{-3} and 10^{-7} cm/s. Therefore, these materials' permeability ranges from low (in an aquifer) to impervious (in an aquifuge).

Several secondary processes significantly increase the effective porosity of a material. These include secondary dolomitization, provided it takes place when the sediment has been consolidated; otherwise, it has very little effect. In this case, the change from calcite to dolomite creates 13% of the rock's total porosity. Porosity is reduced by recrystallization and is enhanced by selective leaching processes.

At least four types of porosities are usually recognized ([10], Table 1.3), depending on the nature of the voids likely to store gravity water. *Microscopic voids* between the minerals generate an *intercrystalline porosity* of up to 0.1–1% of the rock's total porosity. Voids between cemented grains create what is known as *interstitial porosity*. In this way, some types of limestone (oolitic, for example) have an interstitial porosity similar to that of a sandstone. The *porosity of microfissures* corresponds to the voids created mostly by microcracks, diaclases, stratification

Table 1.3 Classification of voids and types of porosity

Scale	Void		Porosity type
Microscopic	Pores or interstices	Intercrystalline	Intercrystalline
		Intergranular	Interstitial
	Microfissures	Stratification joints	Microfissures
Macroscopic		Conduits	Conduits

joints and schistosity. *Macroscopic porosity* refers to large karstified conduits, channels and caves, where fractures have been preferentially exploited by karstification; a specific case is *cavernous porosity*, where holes of karst origin predominate [11].

The first three porosities described above can be generically grouped under the heading of *matrix* porosity, as opposed to *conduit* porosity and that derived from *fractures*. Classical studies of petroleum geology conclude that the greatest total porosity is seen in highly recrystallized calcilutites, followed by pisolitic uncemented limestone, bioclastic limestone with a dolomitic microgranular matrix (15%), oolitic microgranular dolomitic matrix limestone (12%) and microcrystalline dolomite (11%). Values below 2% correspond to micritic limestone and all well-cemented variants.

1.4.2 Porosity and Permeability in Dolomites

1.4.2.1 Types of Porosity in Dolomite

Dolomitization Porosity

Dolomite, in general, is a porous and permeable rock and hence is both a good aquifer and an oil storage rock. Most dolomites are secondary rocks, formed from pre-existing limestone by replacement of part of its Ca by Mg. In the natural environment, *direct precipitation* of dolomite, to create *primary dolomite*, is almost non-existent. The few known examples, of limited extent, are in warm, shallow lagoons that are supersaturated in Mg^{2+} , supratidal plains along extremely arid coasts, known as *sabkhas*, and hypersaline lakes. Replacement dolomite, on the other hand, is generated throughout diagenesis from its earliest to its latest stages and can either affect the entire mass of sediment and/or original limestone rock or take place selectively. In the absence of any extra contribution of carbonate ions and calcium ions to the starting content of the limestone, the mole-by-mole replacement causes a reduction in volume of about 13%, as dolomite is denser than calcite (2.866 compared to 2.718 g/cm³). This results in an increase in the porosity of the resulting dolomitic rock. This type of porosity, known as **dolomitization porosity**, is *intercrystalline* (Fig. 1.3), and the rock consists of a network of partially interpenetrated and relatively well-formed dolomite rhombuses in a structure known as ‘saccharoid dolomite’ or ‘sugar dolomite’.

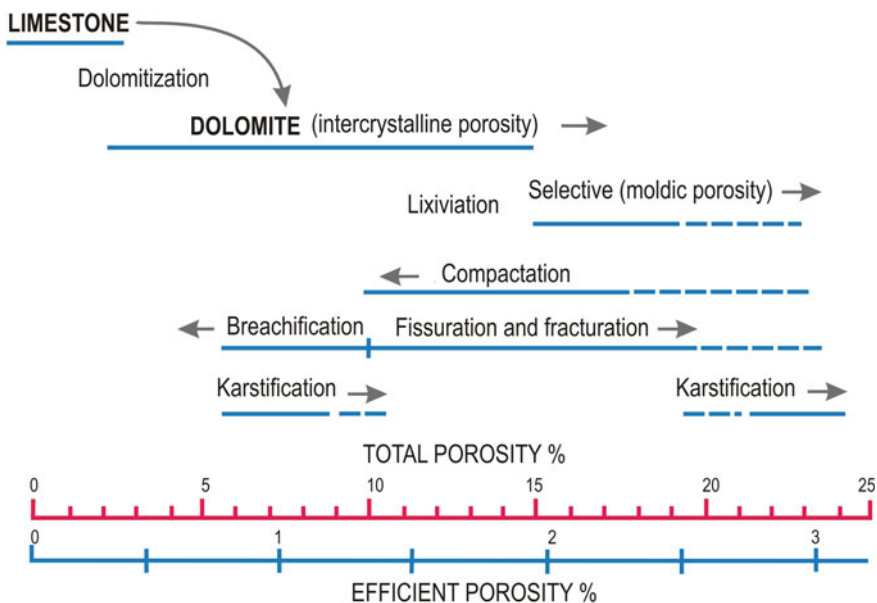


Fig. 1.3 Conceptual scheme of the development of dolomite's porosity as a function of a series of processes (Adapted from [12])

Also of great interest is the porosity that arises during dolomitization by *selective lixiviation* of some textural elements of the original limestone, due to the fact that the dolomitizing fluid is initially undersaturated or partially subsaturated with bicarbonate ions. This type of porosity is *moldic* and very similar in magnitude to its effective porosity. There are good examples in the Betic Cordillera [13] in the ochre dolomite of the Prebetic Upper Cretaceous and the dolomitized reefs of the Mediterranean Messinian. In the first, the presence of dissolution voids formed by preferential lixiviation of some types of fossil fragments (bioclasts) during dolomitization confers a high porosity on the rock, from 5 to 20% of its total volume.

In the example of the Messinian reefs, the porosity caused by the lixiviation of textural elements of the aragonite's original composition, which takes place throughout dolomitization, adds to the reef's initial porosity, for example that inherent in the bio-building framework and the coral breccia of its upper slopes. When the two are combined, the porosity can be greater than 20% of the rock's overall volume. In general, the open spaces in the original limestone are usually preserved in all dolomitization, resulting in high porosity values when added to that created by dolomitization processes.

Frequently, the porosity caused by dolomitization, especially intercrystalline porosity, is significantly reduced or even cancelled out by subsequent **compaction**. This is especially the case when there has been incomplete dolomitization, as the

lattice of dolomite crystals does not then offer enough rigidity to counteract the compaction. Late **cementations**, often of sparitic calcite, may also reduce porosity.

Fracture Porosity

Dolomites are fragile rocks and often appear highly fractured in outcrops, crossed by a multitude of small fissures. The extent of the increase in porosity from this fracturing is easily quantifiable. However, if it is very intense, the rock breaches (Photos 1.1 and 1.2). Such is the case of the *Alpujarrides* dolomite, widespread in the southern provinces of Malaga, Granada and Almería, which has very low permeability values. It seems that once a threshold has been reached, the dolomite breaks and its porosity and permeability do not so much increase as diminish considerably.

Karstification Porosity

Dolomite terrain can be a karst aquifer. The karstification of dolomite, which exploits the previous openings, as in limestone, has the effect of considerably widening any cracks and effectively increasing the rock's porosity. Dolomitic rocks are soluble. Although dolomite is more soluble than calcite and Mg is more soluble than Ca, dolomitic outcrops are leached less than limestone, because dolomite karst water soon becomes saturated and does not precipitate dolomite as speleothems. In limestone, on the other hand, although saturation point is reached temporarily in the

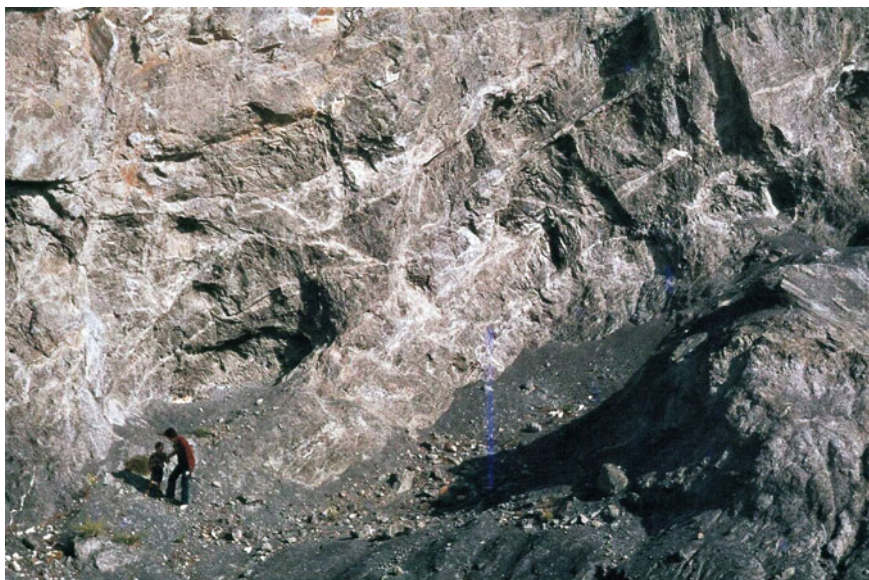


Photo 1.1 Crushed dolomites or *kakititas* of the western edge of Sierra Nevada, used as building material (Photo A. Pulido)



Photo 1.2 Detail of another brecciated dolomite (Creu formation, Valencia; Photo A. Pulido)

karst water, it precipitates calcite frequently as speleothems in caves and other cavities, thus returning to a subsaturated state that can again dissolve the rock.

When karstification is selective and acts on partially dolomitized limestones or partially calcified—de-dolomitized—dolomite, *carniolar structures* develop. In the Betic Cordillera, the most important *carniolar* outcrops are at the base of the Lower Liassic dolomite, and they constitute very interesting aquifers. These particular *carniolar* outcrops correspond to ancient dolomitic rocks that have been partially de-dolomitized by waters rich in calcium sulphate from the leaching of evaporites (gypsum) from the underlying Keuper. Subsequent erosion has acted differentially, releasing the dolomitic portions that were more soluble and mechanically less resistant, giving rise to its characteristic vacuolar structure.

1.4.2.2 Permeability

The permeability of dolomite is very variable, as it is a function of many factors, but is generally considered to be far more constant than in limestone terrain. Extensive data have been obtained from oil research, which regards dolomite as a good rock store. The highest permeability values are observed in dolomites with a high porosity—whether moldic or saccharoid, and fissured—that are unbrecciated and also strongly karstified (Fig. 1.3). The highest values, at over 1000 millidarcies, are seen in highly crystalline dolomite.

1.5 Porosity and Permeability in Matrix

The investigation of the hydrogeological properties of carbonate material can help to establish a conceptual model of such aquifers. In any conceptual model, the matrix plays an important role, especially with regard to the time taken to empty an aquifer, the extent of its residual saturation and the time for it to replenish itself, in the case of an overexploited aquifer [14, 15]. Probably, the main importance of matrix is to the identification of any pollution of the aquifer and subsequent correction [16].

Conceptual models of carbonate aquifers [17–19] often ignore the role of matrix or consider it to be minor, laying more emphasis on fractures and subsequent karstification. However, hydrodynamic and/or hydrogeochemical anomalies are best understood by taking into account the matrix, and the interpretation of a tracer test [20, 21] is quite different if its porosity is considered. For these reasons, studies to evaluate the hydrogeological properties of carbonate matrix are of considerable interest [22].

To illustrate such research, after examining the analysis of fractures, we will comment on two studies on the matrix of carbonate rocks: one on the Devonian of the Olkusz region [22] and one on the Betic Cordillera [23, 24], also the sector south of Ronda, Malaga, the Sorbas gypsum and the Sierra Gorda (see Boxes 1, 2, 3, 4 and 5).

1.6 Fracture Analysis

1.6.1 Basic Concepts

Discontinuities are the points of access and initial circulation of groundwater, in which fracturing and fissures play a key role (Photo 1.3). For this reason, it is interesting to carry out a detailed study of fracturing.

The methodology comprises at least two aspects:

- Location of fractures on aerial photo. Depending on the scale (flight height), the information comes from large alignments, medium alignments or small to very small fractures. While there is a marked subjective component, the method yields valid statistical results. The subsequent study technique can be manual, using ‘optical filtering’ (optical bench), or digital, which is most common currently. It is possible to work either with the frequencies of the trends, with lengths being added on the basis of their direction, or with the separation between fractures, essentially. Fracturing can be shown to be a random variable with a structural component.
- To achieve the correct interpretation, the work on aerial photo has to be complemented by measures on the ground. Aerial photo indicate only the line of a structure’s intersection with the topography, with no clues to its dip, so

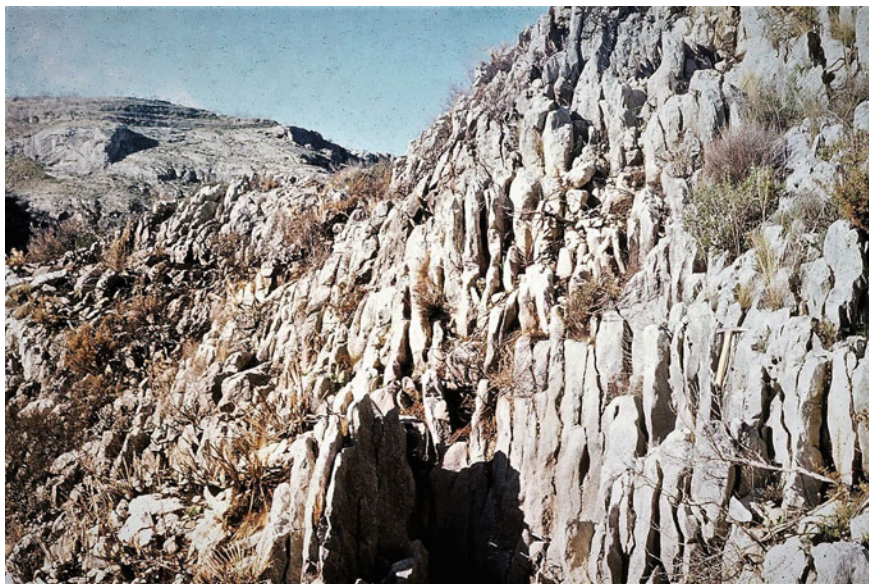


Photo 1.3 Detail of dense fracturing in the Creu formation in Barranco del Infierno, beside the River Serpis (Valencia. Photo A. Pulido)

quarries and either natural or artificial *galleries* are an invaluable source of this information.

In areas of little tectonic complexity, the study of associated minor structures—stylolites, stress cracks and fault drag—alongside photogeological study can determine the angle of the stress ellipsoid. Studies have shown that fracture orientation is uniform across wide areas and is maintained at depth, and that, the frequency of fractures of the same alignment depends upon lithological heterogeneity—the presence of alternating marl strata, for example—and on the thickness of the strata: the less the thickness, the greater the fracture density.

On the other hand, water circulation is not directly related to the density of the fractures so much as to the density of fractures that have had one or more episodes of tension (opening) in their history, provided that clogging and compaction are not involved. The development of fissures guarantees a physical continuity in the circulation environment, permitting the presence of *aquifers* in a carbonate terrain. Karstification processes are superimposed on this underlying framework, further developing a set of *open* fractures to the detriment of others and generating block structures of very varied size as a function of the fracturing. This can be at the scale of tens or hundreds of metres across, or kilometres wide.

Wittke and Louis demonstrated that $k = \frac{gd^3}{12\nu}$ where g = gravity acceleration; d = fissure opening; and ν = kinematic viscosity. This aspect is fundamental, since

it is not so much the fractures' number, orientation and frequency as their separation that is the key, to the extent of the power of three. Furthermore, separation determines not only the k -value but also the type of flow, whether laminar or turbulent, parallel or otherwise, and the water circulation. For example [18], given that suction relies on the narrowness of fissures, controlled by surface tension, the height at which suction operates varies from 300 cm for fissures 5 microns across, 150 cm for cracks 10 microns wide and only 0.15 cm for openings of 1 cm, as these last permit turbulent flow.

Kiraly [25] proposes an expression to estimate the value of permeability k as a function of the frequency of each family (f_i) and the separation of fractures (d), taking into account the matrix identity $I k = \frac{g}{12v} \sum f_i d_i^3 [I - n_i * n_i]$. For his part, Müller proposes the expression $me = \sum f_i d_i$ to estimate the effective porosity (me) according to the frequency of each family (f_i) and fractures' separation (d_i). Rats [26] establishes a relationship between interfractural separation (d) and the thickness of strata (e), arriving at the logarithmic expression $\log d = a + b \log e$, with $a = -0.64$; $b = 0.41$.

To illustrate the above, we will apply fracture analysis to the karst aquifers of the Serranía de Ronda [27] (Box 3) and the Sierra Gorda aquifer [28, 29] (Box 4), with the simple intermediate example of the Sorbas gypsum [30].

1.6.2 Box 1: Olkusz Region (Poland)

Hydrogeological investigations were carried out on samples from four boreholes in the Klucze region (Fig. 1.4), about 8 km north of Olkusz. Samples from the different boreholes were taken at depths of between 180 and 500 m. The samples are mainly limestone and dolomite (Muschelkalk facies) and Jurassic, with only one sample of marl. The diameters of the sample cores were between 46 and 47 mm, and their heights between 47 and 56 mm.

Interconnected porosity (P_0), the total volume of interconnected pores (equivalent to total porosity) and the storage coefficient (S ; *specific yield*) (effective porosity, actually) were measured in 127 samples of limestone, 37 of dolomite and one of marl. Permeability (k) was measured in 126 samples of limestone and 37 of dolomite. The k -values were calculated in the samples using air as the fluid, so they were later recalculated for water at a temperature of 10 °C.

A vacuum chamber was used to measure the open porosity by extracting all the air from the sample and filling the empty space with water while carrying out a series of measurements of its weight. This evaluates the volume of interconnected pores. Prior to going in the vacuum chamber, the samples are dried for at least 24 h in an oven between 105 and 110 °C. The following formula [31, 32] is used to calculate the open porosity coefficient (P_0):

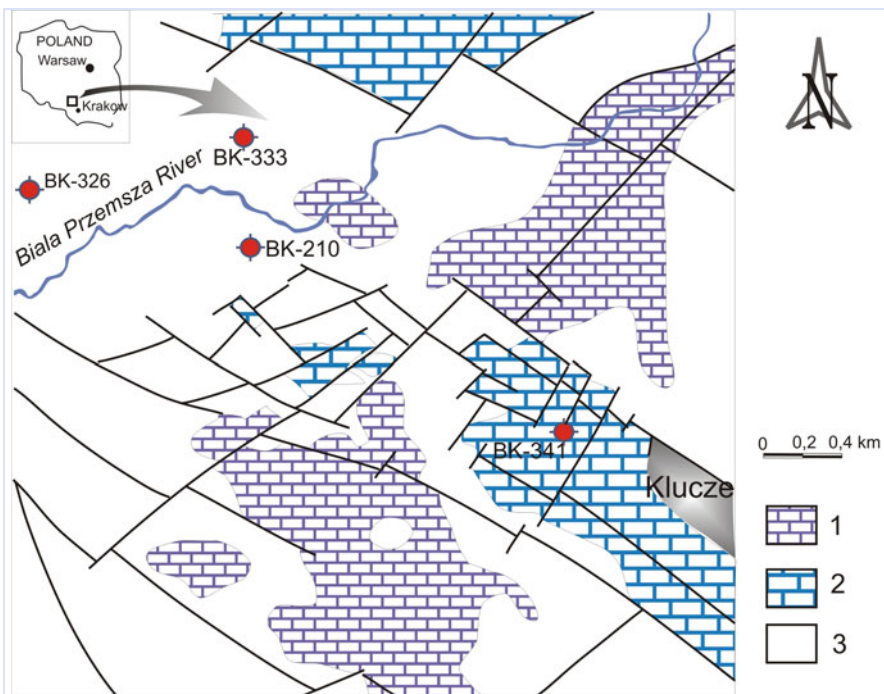


Fig. 1.4 Location of the boreholes studied

$$P_0 = \frac{G_n - G_s}{G_n - G_{nw}} \quad (1.1)$$

where G_n is the weight of the water-saturated sample, G_s the weight of the sample dried at 105–110 °C, G_{nw} is the weight of the water-saturated sample, weighed into the water—using Archimedes principle.

The methodology used to calculate the storage coefficient (S) uses a centrifuge to extract water to accelerate the task, as the natural release of gravity water is a very slow process. The suction pressure exerted on the sample by centrifugal force releases a certain part of the total volume of water contained in a sample (known as gravity water), which is calculated by the following formula:

$$H = \frac{\left(\frac{2\pi n}{60}\right)^2 r h}{g} \quad (1.2)$$

where H is the water suction pressure of the matrix, expressed in metres of height of the water column; n is the number of revolutions per minute; r is the centrifuge radius (distance in m from the axis of the centrifuge to the centre of

gravity of the sample); h is the length of the sample in m; and g is the acceleration of gravity (9.81 m/s^2). The challenge is to set the appropriate suction pressure to simulate natural conditions; in this method, it is the equivalent of a 10 m high water column. The rock's storage coefficient is based on the quantity extracted. Determining the variables ($H = 98 \text{ kPa}$ and length of each sample) derives the number of revolutions to be applied, and the volume of water obtained from the centrifuge is then used to calculate the storage coefficient (S):

$$S = \frac{V_w}{V_r} \quad (1.3)$$

where V_w is the volume of water released for a suction pressure equivalent to a water column 10 m high (cm^3) and V_r is the volume of rock (cm^3). The simulated water extraction pressure in the centrifuge for small samples is equivalent to the maximum water extraction pressure in nature by the action of gravity on a stratum of thickness h .

Centrifugal acceleration (a) is expressed as

$$a = \omega.R^2 \quad (1.4)$$

where a is centrifugal acceleration and ω angular velocity. Working with Eq. 1.2, we arrive at:

$$\frac{H}{h} = \frac{a}{g} \quad (1.5)$$

and also:

$$a = \left(\frac{2\pi n}{60}\right)^2 r \quad (1.6)$$

so that n (no. of revolutions per minute) can be calculated for each sample. According to Prill et al. [32], the relationship between the time for the percolation of gravity water in nature (T_n) and the time spent in the centrifuge (t) can be expressed by:

$$\left(\frac{T_n}{t}\right) = \left(\frac{a}{g}\right)^2 \quad (1.7)$$

All samples were centrifuged for 30 min (T) which, depending on their length, is equivalent to a percolation time under natural conditions (T_n) of between 660 and 940 days (from 2 to 2.5 years). To verify that 30 min is sufficient to allow the removal of the gravity water from the sample, a group of 25 samples were tested; the rest did not release anything in the centrifuge.

As a result, 21 of the sample's results lay between the fastest and slowest graphs, while the remaining four gave virtually no water. Thus, the process takes a maximum of 11 min.

A new parameter known as relative drainability (S_0) can be defined:

$$S_0 = S/P_0 \quad (1.8)$$

as the quotient of the storage coefficient (S) and the open porosity coefficient (P_0). This gives an idea of the diameter of the pores of the matrix, as well as their nature (fissured or small capillary, among others).

For permeability analysis, samples are dried at 105–110 °C and then put into the air permeameter. The expression that allows the calculation of Darcy's permeability coefficient (K_g), expressed in darcys, is as follows:

$$K_g = \frac{2 \cdot Q_0 \cdot P_0 \cdot L \cdot \eta}{F \cdot (p_1^2 \cdot p_2^2)} \quad (1.9)$$

where Q_0 is the gas flow (cm^3/sg); p_0 is the atmospheric pressure (atm); L is the length of the sample (cm); η is the dynamic viscosity coefficient of the gas; F is the sample section (cm^2); p_1 is the gas pressure before passing through the sample (atm); and p_2 is the gas pressure after passing through the sample (atm). The coefficients obtained are then recalculated for water at 10 °C temperature (K_{10}), according to the equation:

$$K_{10} = K_g \frac{\gamma}{\eta} \quad (1.10)$$

where γ is the specific weight of the water. After considering this, we arrive at:

$$K_{10} = 7.66 \times 10^{-6} K_g \quad (1.11)$$

However, the permeability calculated using this formula does not correspond to that which would be obtained naturally and using water. The *Klinkenberg correction coefficient*, which depends on many factors and is inherent to each type of rock, must therefore be employed. Consequently, we know that K_g and the recalculated for water (K_{10}) are in fact lower, especially in samples with low permeability.

The investigated samples were described in terms of microscopic features and by simple field methods. They are usually limestone and dolomite. Depending on their macroscopic structure and texture, the following types can be distinguished, with the number of samples of each in brackets: micritic limestone (39); fissured micritic limestone (58); conglomerate limestone (30); brecciated and fissured dolomite (32); recrystallized dolomite (5); and marl

(1). In fissured or fractured rocks, the filling is calcite. Many fractures, especially in the limestone, are filled with yellowish clay. Seven of the samples show the presence of stylolites [22].

The Devonian limestone of the Klucze region has relatively low open porosity. Its value varies between 0.00185 and 0.064. The mean is 0.0152, the standard deviation 0.014 and the coefficient of variation 0.92. The fissured, micritic and conglomerate limestone has the highest porosity, with the same average porosity. The lowest porosity is seen in the brecciated limestone.

The distribution of the values of open porosity is not homogeneous; there are two subgroups of a dissimilar distribution (Fig. 1.5). The first subgroup includes rocks that show a very low porosity, and the second those that have a slightly higher porosity. Open porosity in the dolomite is generally lower than in the limestone and varies between 0.00212 and 0.0259. The arithmetic mean is 0.0108, the standard deviation 0.00663 and the coefficient of variation 0.61. The highest porosity value is found in the brecciated dolomite with filled fissures. The crystallized dolomite shows a lower value, and the dolomitic breccia lower again. The distribution of open porosity in the dolomite is more homogeneous than in the limestone (Table 1.4). The only sample of a marl has an open porosity value of 0.181, which is higher than that of the limestone and dolomite.

The storage coefficient obtained for the Devonian limestone is very low: only seven of the 127 samples released traces of water. It varies between 0.00064 and 0.00163, and the mean is 0.000065. Although all 127 samples provided water, there are differences between the mean S values for the types of rocks described. The highest S value is shown by the micritic limestone with filled fissures and brecciated limestone, with an average value of

Fig. 1.5 Cumulative frequencies of porosity values

